Chemistry & Biology 13, 637–647, June 2006 DOI 10.1016/j.chembiol.2006.04.008

Heterologous Expression, Purification, Refolding, and Structural-Functional Characterization of EP-B2, a Self-Activating Barley Cysteine Endoprotease

Michael T. Bethune,[1] Pavel Strop,[2] Yinyan Tang,[3] Ludvig M. Sollid,[4] and Chaitan Khosla[1,3,5,*]
[1]Department of Biochemistry
Stanford University
Stanford, California 94305
[2]Howard Hughes Medical Institute and
Departments of Molecular and Cellular Physiology,
Neurology and Neurological Sciences and
Stanford Synchrotron Radiation Laboratory
Stanford University
Stanford, California 94305
[3]Department of Chemistry
Stanford University
Stanford, California 94305
[4]Institute of Immunology
University of Oslo
Rikshospitalet University Hospital
N-0027 Oslo
Norway
[5]Department of Chemical Engineering
Stanford University
Stanford, California 94305

Summary

We describe the heterologous expression in *Escherichia coli* of the proenzyme precursor to EP-B2, a cysteine endoprotease from germinating barley seeds. High yields (50 mg/l) of recombinant proEP-B2 were obtained from *E. coli* inclusion bodies in shake flask cultures following purification and refolding. The zymogen was rapidly autoactivated to its mature form under acidic conditions at a rate independent of proEP-B2 concentration, suggesting a *cis* mechanism of autoactivation. Mature EP-B2 was stable and active over a wide pH range and efficiently hydrolyzed a recombinant wheat gluten protein, α2-gliadin, at sequences with known immunotoxicity in celiac sprue patients. The X-ray crystal structure of mature EP-B2 bound to leupeptin was solved to 2.2 Å resolution and provided atomic insights into the observed subsite specificity of the endoprotease. Our findings suggest that orally administered proEP-B2 may be especially well suited for treatment of celiac sprue.

Introduction

Celiac sprue is a widespread but underdiagnosed autoimmune type enteropathy of the small intestine that is induced by the ingestion of gluten proteins found in cereals such as wheat, rye, and barley. Genetically susceptible individuals develop an inflammatory response to proteolytically resistant, proline- and glutamine-rich epitopes in gluten, resulting in villous atrophy, crypt hyperplasia, and malabsorption of nutrients [1, 2]. The only effective treatment currently available to a patient is strict dietary exclusion of gluten-containing products. Several recent studies have highlighted the therapeutic potential of orally administered prolyl endopeptidases (PEPs), a family of enzymes with the unique ability to cleave at internal Pro residues in proteolytically resistant gluten epitopes [3–8]. However, the effectiveness of these enzymes may be limited by their substrate chain length restrictions [9, 10] and by the fact that they act at the relatively neutral pH of the small intestine, where undigested peptides can simultaneously access the gut-associated lymphoid tissue underlying the intestinal mucosal epithelium. As gluten is comprised of ~35% Gln, a residue that is not a preferred cleavage site for any pancreatic endoprotease, the digestive efficacy of PEPs could be enhanced by coadministration of a Gln-specific endoprotease, particularly if this endoprotease is active upstream of the intestine in the acidic stomach. Here, we describe the heterologous expression, purification, refolding, and structural-functional characterization of a candidate enzyme that fulfills these criteria, the barley cysteine endoprotease, EP-B2.

Our choice of barley (*Hordeum vulgare*) EP-B2 was influenced by the evolutionary argument that nature may have evolved this enzyme to incorporate many desirable characteristics of an oral therapeutic agent that breaks down dietary gluten in the stomach and upper small intestine. EP-B2 is secreted as a proenzyme (proEP-B2) into the acidic endosperm of germinating barley seeds, where it is activated to its mature form. Its physiological substrates are Pro- and Gln-rich hordeins, which are major storage proteins in barley gluten [11–13]. Substrate specificity analysis of EP-B2 purified from green malt barley suggested that EP-B2 cleaves preferentially after Gln residues, often with Pro at the P2 position [14]. However, biochemical studies performed to date have utilized EP-B2 from the natural source (germinating barley seeds), which places intrinsic limits on further enzymological, pharmacological, and protein engineering studies. We therefore sought to produce the proenzyme as a recombinant protein in *E. coli* and to characterize its folded form and activation mechanism as well as the structure, activity, and specificity of the mature enzyme. The results of our studies are reported here.

Results and Discussion

Heterologous Expression and Purification of Recombinant ProEP-B2

Native EP-B2 is synthesized in the aleurone layer of germinating barley seeds as a 43 kDa preproenzyme, possessing a signal sequence that directs the secretion of the proenzyme and is subsequently removed, as well as an N-terminal propeptide that renders proEP-B2 stable and inactive [12]. Previous attempts to express papain-like cysteine proteases in heterologous systems have shown that the signal sequence must be removed prior to heterologous expression [15] and that the propeptide must be retained for proper folding and stability [16–19]. By expressing a truncated form of the *EPB2*

*Correspondence: khosla@stanford.edu

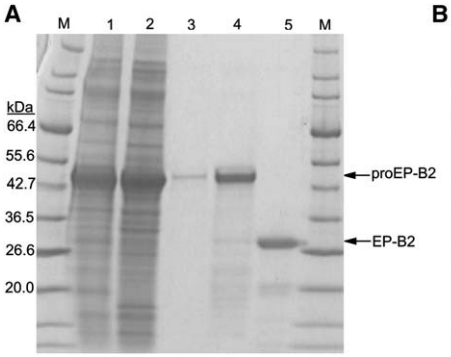

B

MGSSHHHHHHSSGLVPRGSHMASMT
GGNNMGRDPCSAIPMEDKDLESEEAL
WDLYERWQSAHRVRRHHAEKHRRFG
TFKSNAHFIHSHNKRGDHPYRLHLNRF
GDMDQAEFRATFVGDLRRDTPSKPPS
VPGFMYAALN▼VSDLPPSVDWRQKG
AVTGVKDQGKCGSCWAFSTVVSVEGI
NAIRTGSLVSLSEQELIDCDTADNDGC
QGGLMDNAFEYIKNNGGLITEAAYPYR
AARGTCNVARAAQNSPVVVHIDGHQD
VPANSEEDLARAVANQPVSVAVEASG
KAFMFYSEGVFTGECGTELDHGVAVV
GYGVAEDGKAYWTVKNSWGPSWGEQ
GYIRVEKDSGASGGLCGIAMEASYPVK
TYSKPKPTPRRALGARESL**NSSSVDKL**
AAALEHHHHHH

Figure 1. Purification and Sequence of Recombinant ProEP-B2

(A) SDS-PAGE analysis of NiNTA column purification of proEP-B2. Lanes: molecular weight markers (M); resolubilized inclusion bodies (1); NiNTA column flowthrough (2); NiNTA column wash (3); NiNTA column eluate (4); and mature EP-B2 following proEP-B2 purification, refolding, and activation at pH 4.5 (5).

(B) Sequence of recombinant proEP-B2. Recombinant proEP-B2 is 43.7 kDa. Plasmid contributions are in bold; residues altered by primer-directed mutagenesis for cloning are underlined. Mature EP-B2 is 27.7 kDa. The N terminus of mature EP-B2 (▼) was determined by N-terminal sequencing.

gene lacking its signal sequence, an expression level of 50 mg of recombinant, His_6-tagged proEP-B2 per liter of *E. coli* culture was achieved. The majority of this polypeptide was recovered in the pellet from high-speed centrifugation of the cell lysate, suggesting that proEP-B2 was expressed predominantly in inclusion bodies. This is a common fate for papain-like cysteine endoproteases expressed in heterologous hosts [20]. Following denaturing nickel-nitriloacetic acid (Ni-NTA) affinity chromatography, a single major band eluted from the column at ~45 kDa with a purity of >90%, as assessed by SDS-PAGE (Figure 1A). This is in good agreement with the predicted molecular weight (43.7 kDa) of recombinant proEP-B2 based on its sequence (Figure 1B).

The purified material was refolded by rapid dilution into a refolding buffer at pH 8.0, yielding folded proEP-B2, as measured by its ability to self-activate into a single 30 kDa product under acidic conditions (Figure 1A, lane 5). N-terminal sequencing of this product revealed that it corresponded to a 27.7 kDa mature EP-B2 protein (Figure 1B). The N terminus of this recombinant mature enzyme includes a two-residue extension compared to the naturally derived mature enzyme [12], a feature that has precedence in the context of other recombinant cysteine endoproteases activated in vitro [20].

Crystallization and Structure Determination of Mature EP-B2 Bound to Leupeptin

To provide a structural basis for the mechanism of activation of EP-B2 and its hydrolytic activity toward specific peptide sequences, we solved the X-ray crystal structure of EP-B2 complexed with the peptidic cysteine protease inhibitor, leupeptin. Following activation of proEP-B2 to its mature form and covalent inhibition with leupeptin, the EP-B2-leupeptin complex was purified by FPLC and crystallized by hanging drop vapor diffusion. The complex crystallized in the space group P1 with four covalently inhibited EP-B2 monomers per asymmetric unit. The crystal structure was solved by molecular replacement and refined to 2.2 Å resolution with R and R_{free} values of 20.3% and 23.3%, respectively. Data, refinement, and model statistics are shown in Table S1 (see the Supplemental Data available with this article online).

The overall structure of mature EP-B2 consists of two comparably sized domains, canonically designated R and L, which are divided by the active site cleft (Figure 2A). Numbering from the N terminus of the mature recombinant enzyme (Figure 1B), domain R is primarily composed of an extended N-terminal loop (residues 3–23) and four antiparallel β sheets (residues 121–223), while the predominantly α-helical domain L comprises residues 24–120 and the observed C-terminal residues 224–226. Three conserved disulfide bonds (Cys25-Cys67, Cys59-Cys100, Cys161-Cys213) further stabilize EP-B2's tertiary structure, which shares a high degree of similarity to previously determined structures of related cysteine endoproteases (Figure 2B). Residues 1–2 and 227–262 of the mature enzyme are not well defined by the electron density and are not included in the refined model.

The active site of EP-B2 is located within an ~10 Å deep groove that spans the junction between the R and L domains (Figure 2C). The main chain of leupeptin is bound along the length of this groove by two hydrogen bonds between Gly70 and the P2 position backbone atoms of the substrate and by a third hydrogen bond between Asp166 and the P1 position backbone. These interactions serve to position the C-terminal aldehyde of leupeptin proximal to the Cys28 thiolate. The side chain of Gln22 and the main chain nitrogen atoms of Ser27 and Cys28 comprise the oxyanion hole, which stabilizes the negative charge buildup on the carbonyl oxygen of the substrate upon Cys28-mediated nucleophilic attack. As in other cysteine proteases, the nucleophilicity of the catalytic cysteine is enhanced by His167-mediated proton abstraction (sulfur to nitrogen distance = 3.7 Å). The amide oxygen of the conserved Asn188 side chain orients His167 for proton abstraction from Cys28 (O-N distance = 2.9 Å), thus completing the catalytic triad (Figure 2D).

The substrate specificity of cysteine endoproteases is substantially influenced by enzyme interactions with substrate residues beyond those P1 and P1′ residues flanking the scissile bond (e.g., substrate residues in contact with the S3–S2′ subsites) [26]. Leupeptin, a tripeptide cysteine protease inhibitor, occupies the S3–S1 subsites of EP-B2, allowing for identification of those enzyme residues that participate in binding substrate residues located N-terminal to the site of cleavage (Figures 2C and 2E). In contrast to the related cysteine endoprotease, papain, where two tyrosine residues restrict the size of P3 side chains [26, 27] (Figure 2E), the S3

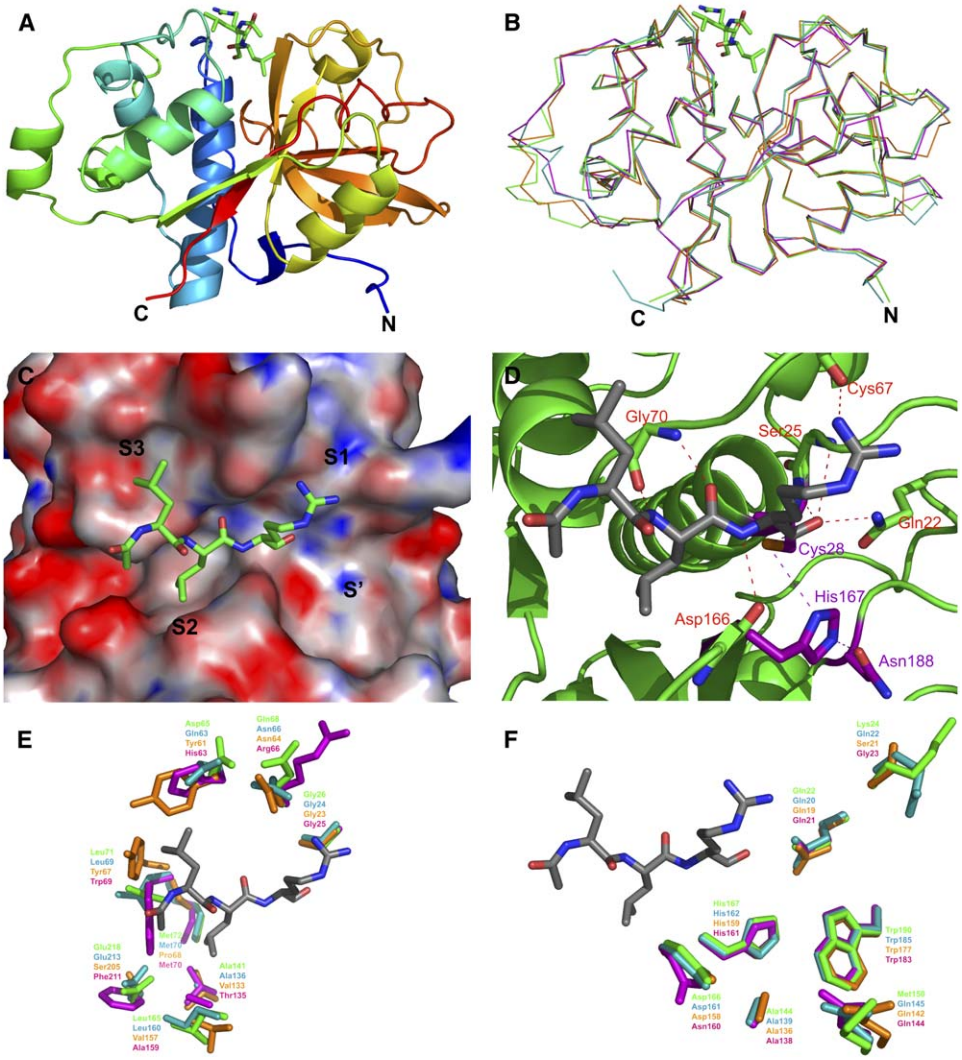

Figure 2. Crystal Structure of Mature EP-B2 Complexed with Leupeptin

(A) Ribbon diagram of EP-B2 monomer bound to leupeptin (acetyl-Leu-Leu-Arg-al). Color-coding of EP-B2 is according to primary sequence, from blue (N terminus) to red (C terminus); inhibitor is shown in green in stick representation. Orientation is the standard view for cysteine endoproteases, with the R domain at right, the L domain at left, and the active site at top.

(B) Cα alignment of EP-B2 (green; PDB ID: 2FO5) with CysEP (teal; PDB ID: 1S4V) [21], papain (orange; PDB ID: 1STF) [22], and GP-II (magenta; PDB ID: 1CQD) [23]. Modifications to active-site cysteines in structures other than EP-B2 have been removed for clarity.

(C) Molecular surface depiction of the EP-B2 active site cleft (top view). The EP-B2 surface is colored according to electrostatic potential (blue, positive; red, negative; white, neutral); inhibitor in green. Potential values shown are in the range of $-25\ k_BT$ to $+25\ k_BT$. Electrostatic potential was calculated with the program APBS [24].

(D) Active site of EP-B2 (top view). Catalytic triad residues (Cys28, His167, and Asn 188) are colored and labeled in purple. Main chains and side chains of EP-B2 residues forming polar contacts with leupeptin (red dashed lines) are shown and are labeled in red. Inhibitor is in gray.

(E and F) Alignment of cysteine endoprotease structures from (B) (same coloring and modifications for clarity) emphasizing those residues comprising the S2–S1 (E) and the expected S1′–S2′ (F) subsites. Residue labels are colored in correspondence to the structural coloration. All figure panels were prepared with the molecular graphics program PyMOL [25].

subsite of EP-B2 features Asp65 and Leu71 at the corresponding positions, thereby yielding a markedly more open pocket. Residues Gly69 and Gly70 lie at the base of this pocket. In addition, the carbonyl oxygen of Asp63 provides the potential for hydrogen bonding with the substrate. The S2 subsite is usually the deepest pocket in cysteine endoproteases [21, 26–28]. In EP-B2, this pocket is lined by predominantly hydrophobic residues, including Leu71, Met72, Ala141, and Leu165, but has the anionic Glu218 residue at its base. As in CysEP [21], the presence of residue Leu71 in place of bulkier aromatic residues, found in many other cysteine endoproteases (e.g.,Trp in GP-II, Tyr in papain), renders this pocket substantially wider in EP-B2. Finally, the S1 subsite consists of a shallow depression between Gly26 and Gly69 as well as the carbonyl oxygen of Cys65, which is presumably available for hydrogen bonding. In papain and *R. communis* CysEP, an Asn residue may additionally interact with the P1 side chain of long polar residues, but the orientation of the corresponding EP-B2 residue, Gln68, renders this interaction unlikely in EP-B2.

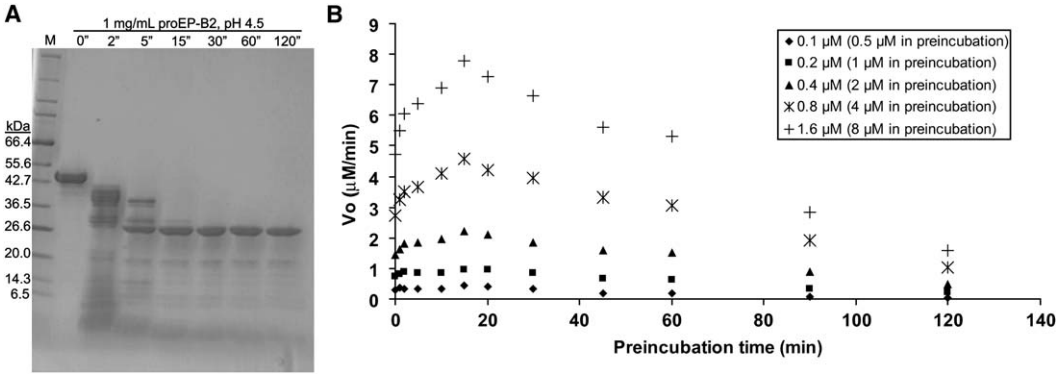

Figure 3. Activation of ProEP-B2 to Mature EP-B2

(A) Time course of proEP-B2 activation. One milligram per milliliter (~23 μM) proEP-B2 was activated for 0–120 min at pH 4.5, 25ºC, and the extent of activation was analyzed by SDS-PAGE. Molecular weight markers (M). Results are typical of more than five similar experiments.
(B) Concentration dependence of proEP-B2 activation. 0.5–8 μM proEP-B2 was preincubated at pH 3.0, 25ºC, for the specified duration, and then chromogenic substrate Z-FR-pNA was added to a final concentration of 50 μM. In the process, a 5-fold dilution of the protein occurs (corresponding to 0.1–1.6 μM preincubated proEP-B2). The reaction rate was measured from the initial slope of the A_{410} versus time plots and converted to Vo in μM/min with ε_{410} = 8,800 $M^{-1}cm^{-1}$ for pNA.

Although the lack of inhibitor residues C terminal to the aldehyde functional group precludes definitive definition of individual subsites in the S′ region of EP-B2, several general observations can be made. First, the S′ region of the active site is wider and less polar than the S region (Figure 2C). Additionally, the identity and orientation of those residues that presumably define the S1′ and S2′ subsites in EP-B2, defined by analogy to the solved structure of cathepsin B with an epoxysuccinyl-based inhibitor bound to its S′ region [29], are strikingly more conserved than those comprising the corresponding S region (Figures 2E and 2F). Together, these points suggest that the S region of the active site cleft plays a more important role than the S′ region in determining EP-B2 specificity, though residues in this latter region may contribute as well.

Kinetics of Activation of ProEP-B2 to Mature EP-B2

In a germinating barley seed, activation of proEP-B2 proceeds through a series of posttranslational processing steps to yield the mature enzyme capable of cleaving hordeins and other cereal storage proteins [12]. Since related cysteine endoproteases autoactivate to their mature forms in vitro when introduced into an acidic environment [30, 31], we sought to determine whether recombinant proEP-B2 can be autocatalytically activated to its mature form under analogous conditions. Recombinant proEP-B2 was therefore incubated in a pH 4.5 buffer, a pH value at which activity of barley-derived EP-B2 has been reported [28]. The extent of activation as a function of time was analyzed by SDS-PAGE. As shown in Figure 3A, under these conditions, proEP-B2 was almost completely activated to its mature form within 15 min, and the full-length proenzyme disappeared by the earliest time point measured (2 min). Interestingly, a series of intermediates are observed between 2–5 min, suggesting that autoactivation involves propeptide cleavage at multiple sites. Similar results were observed in a pH 3.0 buffer (data not shown), highlighting the pharmacological potential for autoactivation of EP-B2 in the acidic stomach. In further support of the hypothesis that proEP-B2 activation is autocatalytic in nature, equimolar addition of leupeptin completely blocked activation over a similar time course (data not shown).

Autoactivation of proEP-B2 can proceed through two nonexclusive mechanisms, *cis* and *trans* activation. If *cis* activation predominates, activation occurs through intramolecular cleavage(s), and the rate of activation should be independent of proEP-B2 concentration. In contrast, if *trans* activation predominates, the rate of activation should increase with proEP-B2 concentration. We therefore preincubated proEP-B2 at varying concentrations in a pH 3.0 buffer. At each concentration, the chromogenic substrate Z-FR-pNA was added at various time points and enzyme activity was measured. As shown in Figure 3B, the enzymatic activity measured immediately upon addition of proEP-B2 (0 min time point) in each curve is proportional to the proEP-B2 concentration in that reaction mixture, suggesting that the rate of proEP-B2 activation is first order with respect to proEP-B2 concentration. Furthermore, the time taken to reach maximum enzyme activity at each proEP-B2 concentration is also independent of proEP-B2 concentration. Together, these observations suggest that proEP-B2 activation occurs primarily via a *cis* intramolecular cleavage mechanism, a feature that is well suited for in situ gastric activation of orally administered proEP-B2 and a mechanism of activation that was not revealed by the previous heterologous expression of EP-B2 in *Trichoderma reesei* [32–34].

Although the above kinetic data support intramolecular activation, the distance between the N terminus of the mature enzyme and the active site is ~30 Å (Figure 2A), suggesting that the cleavage of the peptide bond between the propeptide region and the mature enzyme is intermolecular. We therefore propose a two-step activation mechanism, in which intramolecular activation under acidic conditions is followed by a faster intermolecular cleavage reaction. Such a model is supported by the structures of the zymogen [35] and mature [36] forms of the closely related cysteine endoprotease cathepsin L, as well as related mechanistic observations [37, 38].

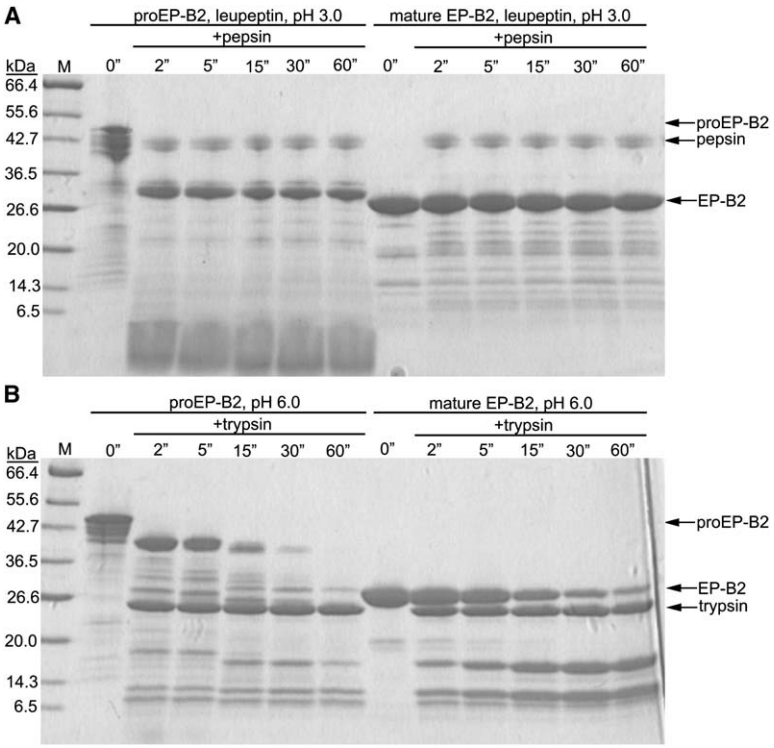

Figure 4. Proteolytic Susceptibility of ProEP-B2 and Mature EP-B2 to Pepsin and Trypsin

(A) Pepsin (0.5 mg/ml) was incubated at pH 3.0 with 0.5 mg/ml proEP-B2 or mature EP-B2 in the presence of 100 M equivalents of leupeptin. At designated time points, the reaction was quenched and the digestion products were loaded on SDS-PAGE. Molecular weight markers (M).

(B) Trypsin (0.5 mg/ml) was incubated at pH 6.0 with 0.5 mg/ml proEP-B2 or mature, inactivated EP-B2, and the reaction progress was monitored by SDS-PAGE. Results are typical of two similar experiments.

In addition to providing insight into the mechanism of proEP-B2 activation, the data in Figure 3B also suggest that mature EP-B2 inactivates slowly, presumably via autolysis at pH 3.0. This is confirmed by SDS-PAGE analysis and can be attenuated in the presence of other preferred substrates of EP-B2 such as gliadins (data not shown).

Comparison of ProEP-B2 and EP-B2 Susceptibility to Pepsin and Trypsin

The therapeutic utility of EP-B2 for celiac sprue would be substantially influenced by its sensitivity to the major proteases of the gastrointestinal tract, pepsin in the stomach, and trypsin and chymotrypsin in the small intestine. We therefore incubated both proEP-B2 and EP-B2 with either pepsin (at pH 3.0) or trypsin and chymotrypsin (at pH 6.0) and analyzed the reaction mixtures by SDS-PAGE. Leupeptin was added to reactions performed at pH 3.0 to prevent self-processing of proEP-B2 to its mature form. In the presence of an equivalent amount of pepsin, mature EP-B2 was highly resistant to proteolysis over a 60 min incubation period (Figure 4A). Pepsin rapidly digested the propeptide region of proEP-B2 but left intact a stable band corresponding to the size of the mature enzyme. In contrast, mature EP-B2 is susceptible to physiological concentrations (0.5 mg/ml) of trypsin with a half-life of ~15 min (Figure 4B) but is resistant to comparable concentrations of chymotrypsin (data not shown). Thus, EP-B2 can be expected to remain active during the gastric phase of gluten digestion but be rapidly broken down in the duodenum. If necessary for its therapeutic application, the intestinal stability of recombinant EP-B2 could be increased through structure-guided modification of susceptible trypsin cleavage sites.

pH Dependence of ProEP-B2 Activation and Mature EP-B2 Activity

For orally administered proEP-B2 to effectively break down dietary gluten in the upper gastrointestinal tract, it must be activated in the acidic environment (pH 2–3) of a fasted stomach and retain high activity in the weakly acidic pH range of the postprandial stomach and duodenum (pH 3–7) [39]. We therefore investigated the pH dependence of zymogen activation as well as of mature EP-B2 activity. When recombinant proEP-B2 was added to Z-FR-pNA in a series of citrate-phosphate buffers ranging from pH 2.3–6.9, the enzyme activity was apparently optimal at pH 4.5 (Figure 5). This observation is consistent with the reported pH optimum of 4.0 determined for the native proenzyme from barley [28] and represents a composite pH optimum for the dual processes of autoactivation of proEP-B2 to mature EP-B2, as well as the catalytic activity of mature EP-B2 against the chromogenic substrate. To determine the pH optimum of each process separately, two additional experiments were performed. First, the pH optimum of proEP-B2 activation was determined by preincubating proEP-B2 over a range of pH values (2.3–6.9) for 30 min, followed by measurement of Z-FR-pNA turnover at pH 6.0. In separate experiments, it was determined that at pH 6.0 mature EP-B2 is active, but no further activation of proEP-B2 will occur. The reaction rate in each sample therefore corresponds to the amount of mature enzyme produced during preincubation under a given pH regime. In the second experiment, the pH optimum of EP-B2 activity was determined by completely activating proEP-B2 at a constant pH of 4.5, followed by measurement of its activity against Z-FR-pNA across a range of pH values. Here, all reactions began with the same amount of active EP-B2, so differences in rates between reactions were

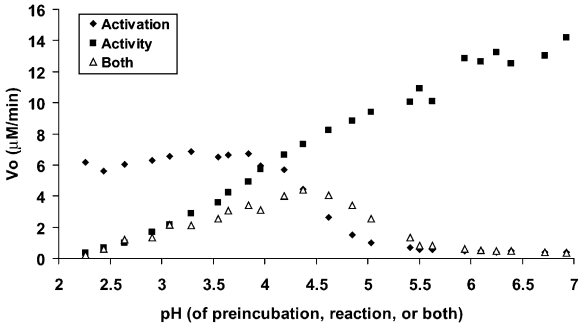

Figure 5. pH Optimum of ProEP-B2 Activation and EP-B2 Activity

To measure pH dependence of autoactivation, proEP-B2 was preincubated 30 min at pH 2.3–6.9 and then assayed at pH 6.0 (◆), a pH value at which autoactivation does not occur to an appreciable extent. To measure pH dependence of mature EP-B2 activity, proEP-B2 was fully activated at pH 4.5 for 60 min and then assayed at pH 2.3–6.9 (■). The composite effect of pH on proenzyme activation and enzyme activity is also shown (△), where substrate was added directly to proEP-B2 at pH 2.3–6.9. ProEP-B2 concentration was 400 nM in all reactions, and 50 μM Z-FR-pNA was used. Vo was calculated as described in Experimental Procedures.

solely due to the effect of pH on the activity of mature EP-B2. As shown in Figure 5, activation of proEP-B2 occurs most efficiently below pH 4.0, but, once activated, the specific activity of mature EP-B2 increases with increasing pH up to pH 7.0. These separate pH optima account for the apparent pH optimum of 4.5 for the combined processes.

In addition to providing new insight into this cysteine protease's remarkable pH dependence, this finding has therapeutic ramifications for celiac sprue. When administered orally into the prefed stomach, proEP-B2 should activate rapidly and then catalyze the breakdown of any dietary gluten that enters the stomach with the meal. Its extreme resistance to pepsin would enable it to survive throughout the residence time of food in the stomach and even continue cleaving residual gluten peptides when the food is emptied in the duodenum. Eventually, EP-B2 will be deactivated by trypsin proteolysis.

Activity of EP-B2 against More Complex Substrates

Although the precise mechanisms underlying celiac sprue pathogenesis remain to be fully elucidated, there exists much evidence that two attributes of gluten peptides contribute to their antigenic potential: their proteolytic resistance [3–5, 10] and their deamidation at selected Gln residues by human transglutaminase 2 [4, 40–45]. Therefore, for barley EP-B2 to accelerate gastrointestinal gluten detoxification, it must have complementary specificity to endogenous proteases. In particular, since neither pepsin nor the pancreatic proteases recognize Gln as a preferred cleavage site (although chymotrypsin has low specificity for Gln), we were intrigued by the possibility that EP-B2 could fulfill this role. To analyze the subsite bias of EP-B2 in the context of representative gluten peptides and proteins, we used two substrates—a Pro- and Gln-rich highly antigenic 33-mer peptide [4] and recombinant α2-gliadin [46], the gluten protein from which this peptide is derived.

The 33-mer peptide, LQLQPFPQPQLPYPQPQLPYPQ PQLPYPQPQPF, bearing six copies of three immunodominant epitopes, was tested because its pharmacological relevance and repetitive sequence make it an ideal target for initial efficacy studies. Incubation of the 33-mer peptide with catalytic amounts of proEP-B2 (1:10 molar ratio, enz:sub) at pH 3.0 for 60 min resulted in substantial breakdown of the peptide (Figure 6A), although the peptide was stable under similar conditions without enzyme added (data not shown). Three major proteolytic fragments were observed by LC-MS/MS analysis (Figure 6B) that collectively identified four cleavage sites within the 33-mer peptide (Figure 6C). Interestingly, the P1 positions of three of these cleavage sites correspond

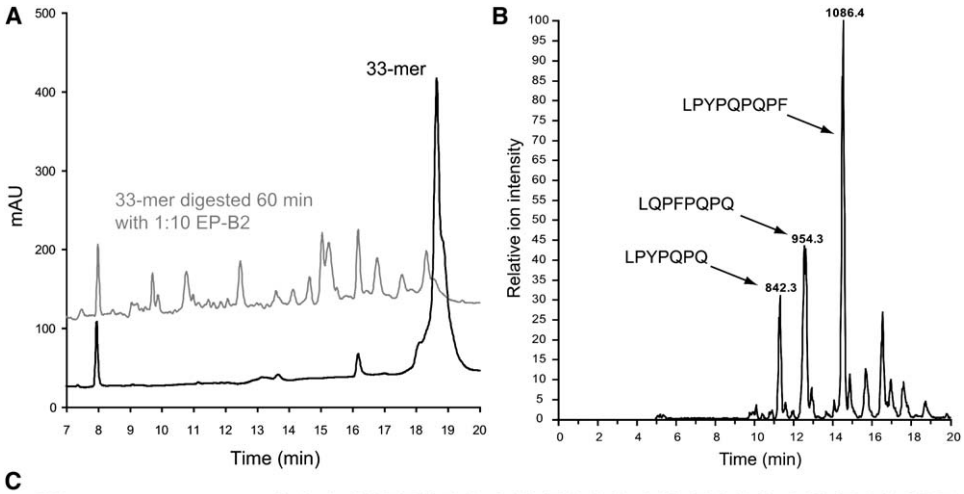

Figure 6. Activity of EP-B2 against the Proteolytically Resistant 33-mer Peptide from α2-Gliadin

(A) RP-HPLC UV_{215} traces of the intact synthetic 33-mer and of 33-mer following 60 min of digestion by EP-B2 at a molar ratio of 1:10 proenzyme:substrate (pH 3.0).

(B) LC-MS mass chromatogram of the digested sample from (A). Peaks labeled as digestion fragments were identified by their MS^2 spectra.

(C) Sequence of the 33-mer peptide showing sites of EP-B2 catalyzed cleavage (↓), as determined by LC-MS/MS.

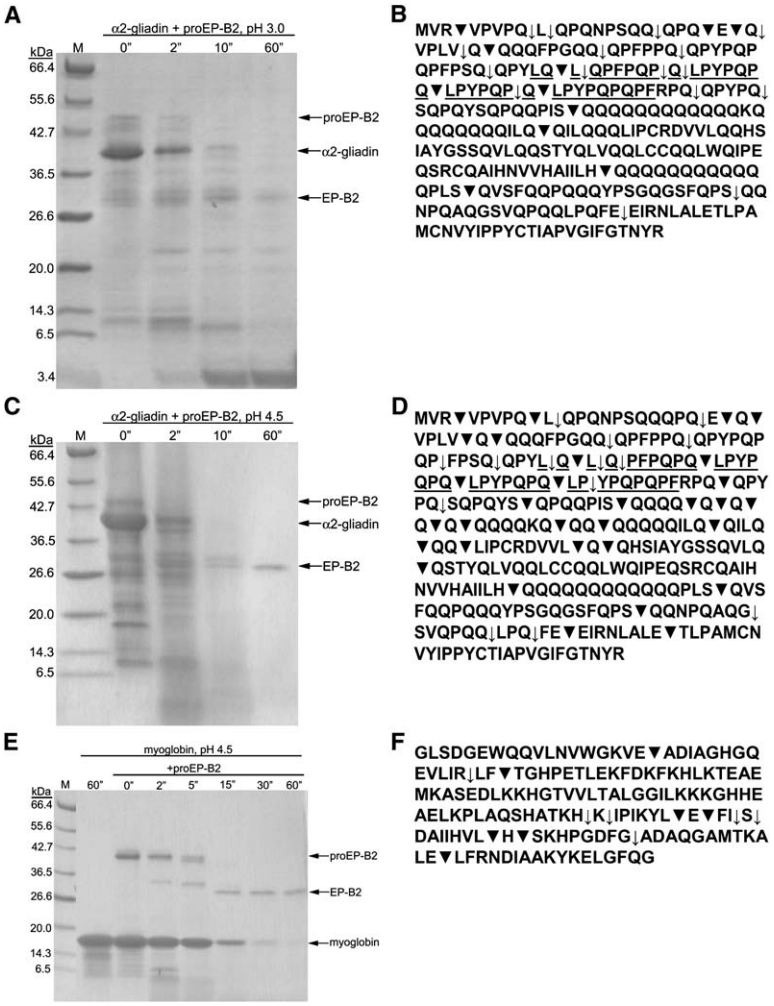

Figure 7. Specificity of EP-B2-Catalyzed Cleavage of the Recombinant Gluten Protein, α2-Gliadin

(A) Time course of α2-gliadin digestion at pH 3.0. ProEP-B2 was added to α2-gliadin at a molar ratio of 1:10 proenzyme:substrate at pH 3.0, and the reaction was allowed to proceed for 60 min. At the indicated times, the reaction was sampled, quenched, and the digestion products were analyzed via SDS-PAGE. Molecular weight markers (M). Results are typical of more than five similar experiments.

(B) Sequence of α2-gliadin showing sites of cleavage as determined by LC-MS/MS following 5 min (▼) or >15 min (↓) incubation with proEP-B2 at a molar ratio of 1:10 proenzyme:substrate (pH 3.0). The sequence corresponding to the 33-mer peptide is underlined.

(C) As in (A), but the digestion was performed at pH 4.5.

(D) As in (B), but from pH 4.5 digestion.

(E) Time course of equine skeletal muscle myoglobin digestion at pH 4.5. ProEP-B2 was added to myoglobin at a molar ratio of 1:10 proenzyme:substrate at pH 4.5, and the reaction was allowed to proceed for 60 min. At the indicated times, the reaction was sampled, quenched, and the digestion products were analyzed via SDS-PAGE.

(F) Sequence of myoglobin showing sites of cleavage as determined by LC-MS/MS following 5 min (▼) or >15 min (↓) incubation with proEP-B2 at a molar ratio of 1:10 proenzyme:substrate (pH 4.5).

to the primary sites of transglutaminase-mediated in vitro deamidation of this antigenic peptide [4]. Extensive analysis of the epitope sequences within the 33-mer peptide [40] indicates that the observed EP-B2 catalyzed proteolytic pattern should result in complete elimination of its inflammatory potential.

Notwithstanding these encouraging results, the observed cleavage sites in the 33-mer peptide provide limited information regarding EP-B2 specificity, since almost all peptide bonds in this sequence contain a typically disfavored Pro residue in the P1 or P1′ positions [28]. To obtain more extensive and pharmacologically relevant insight into the specificity of recombinant EP-B2, catalytic amounts (1:10 molar ratio) of proEP-B2 were incubated with recombinant α2-gliadin, a representative wheat gluten protein, at both pH 3.0 and pH 4.5. At specified time points, the reaction mixture was analyzed by SDS-PAGE or by LC-MS/MS. As shown in Figure 7A, proEP-B2 was able to completely and rapidly hydrolyze α2-gliadin into small peptide fragments at pH 3.0, although the protein was stable under similar conditions in the absence of proEP-B2 (data not shown). Most of these fragments were identified by LC-MS/MS and used to construct a map containing all cleavage sites (Figure 7B). Notably, 11 cleavage sites, distributed unevenly across the sequence of α2-gliadin with most cleavages occurring in the immunogenic, PQ-rich N-terminal region, were identified after only 5 min incubation. After 60 min, 16 additional cleavage sites were detected, again concentrated primarily in the immunogenic region of α2-gliadin. All cleavage sites present in the 33-mer peptide were also identified in α2-gliadin. At pH 4.5, 31 cleavage sites were identified within 5 min in α2-gliadin (Figure 7C), with another 14 identified following more extensive digestion (Figure 7D), making for an average of one cleavage site per 6.4 residues. Cleavage sites were more evenly distributed across the sequence of α2-gliadin at pH 4.5 than at pH 3.0, suggesting that EP-B2 had lower sequence specificity at pH 4.5 than at pH 3.0. Analogous EP-B2-catalyzed digestion of myoglobin, a common dietary protein with lower Pro (3%) and Gln (4%) content, revealed markedly slower degradation (Figure 7E) and fewer cleavage sites (13 sites after 60 min of digestion, for an average of one cleavage site per 11.8 residues; Figure 7F). Together these results suggest that recombinant EP-B2 cleaves preferentially in PQ-rich protein regions, as are present in its natural substrates, the barley hordein proteins, and other immunogenic gluten proteins that precipitate inflammation in celiac sprue.

Since Pro and Gln are the two most abundant residues in gluten (present at ~15% and 30% abundance,

respectively), the overall α2-gliadin cleavage pattern was used to estimate the selectivity for Pro and Gln residues at each subsite (P5 through P5′) in a canonical EP-B2 cleavage site (see the Supplemental Data). This analysis revealed that at both pH 3.0 and pH 4.5, Pro is favored at the P2′ and P4′ positions but is disfavored at the P1′ position, while Gln is favored at the P1, P1′, and P5′ positions. At pH 3.0, further preference is exhibited for sites containing Pro at the P4, P3, and P2 positions. The S2 subsite, a major determinant of cysteine endoprotease specifity [21, 26–28], does not appear to influence strongly the selectivity of EP-B2 for Pro and Gln, perhaps because these amino acids do not form substantial contacts with the relatively wide S2 pocket in EP-B2 (Figure 2E). On the other hand, selectivity for Gln at the P1 position was observed at both pH levels tested, consistent with results obtained for the natural enzyme [28]. The S1 pocket of EP-B2 features a Gln at position 68 (Figure 2E), the identity and positioning of which distinguishes it from the otherwise close structural homolog, castor bean CysEP, which has an Asn at the corresponding position and does not share a strong selectivity for Gln at the substrate P1 position [21]. Since each amino acid position is assumed to be independent of others in this analysis, recurring sequence motifs present in α2-gliadin might cause residues that are unimportant to EP-B2 specificity to appear significant due to their repeated positioning proximal to preferred residues. Nonetheless, EP-B2 cleaves at 61% (11/18) of Q↓XP motifs, compared to 41% (43/105) of Q↓XX residues, suggesting that, minimally, the positioning of proline at P2′ enhances cleavage following glutamine, a subsite preference that is likely general to cysteine endoproteases, given the high degree of sequential and structural conservation in the S′ region (Figure 2F). Remarkably, the EP-B2 consensus sequence (Q↓QPXPQ) overlaps with the consensus sequence of human transglutaminase 2 (**Q**XP, deamidated Gln in bold), an enzyme that plays a critical role in unmasking the inflammatory potential of gluten peptides in celiac sprue [47, 48]. In this issue of *Chemistry & Biology*, an accompanying report from our laboratory describes experiments that evaluate the efficacy of EP-B2 at reducing the antigen burden of grocery-store gluten [49].

Significance

We have developed a heterologous bacterial expression system and a simple purification and refolding procedure for the production of high yields (50 mg/l) of pure, active proEP-B2, the proenzyme form of a major barley cysteine endoprotease. This has enabled us to ask fundamental questions about the mechanism, kinetics, and pH dependence of proEP-B2 activation that were previously intractable using mature enzyme purified from natural or alternative heterologous sources. Additionally, we have structurally and biochemically characterized mature EP-B2 to evaluate its therapeutic suitability as an enzyme supplement for treatment of celiac sprue. We found that proEP-B2 was rapidly autoactivated to its mature form under acidic conditions that are similar to those found in the stomach. Mature EP-B2 was active against the chromogenic substrate, Z-Phe-Arg-pNA, over a wide range of acidic pH values corresponding to the conditions found in postprandial stomach and the upper small intestine. EP-B2 also efficiently digested a recombinant wheat gluten protein, α2-gliadin, as well as a highly immunogenic and proteolytically resistant 33-mer peptide derived from it. Strikingly, the specificity of EP-B2 catalyzed cleavage (Q↓QPXPQ) was found to overlap with the consensus sequence for human transglutaminase 2-mediated deamidation of Gln residues in gluten proteins (QXP), an event believed to be of critical importance in celiac sprue pathogenesis. Our findings suggest that recombinant proEP-B2, perhaps in conjunction with a proline endopeptidase, may be especially well suited for celiac sprue therapy. An accompanying report from our laboratory further evaluates its potential as a gluten-detoxifying enzyme therapy.

Experimental Procedures

Expression and Purification of Recombinant EP-B2

The cDNA for *EPB2* (pHVEP4) was obtained as a gift from T.-H.D. Ho (GenBank accession number: U19384) [1]. Primer-directed mutagenesis was used to introduce a *Bam*HI site upstream of *EPB2*'s proregion, allowing for amplification of a truncated form of the gene lacking its signal sequence. Primers used were 5′-GCGGCCGT GGATCCCTGCAGCG-3′ and 5′-CGATCGATCAGTGAATTC-AGTGA CTCCCTGGCTCC-3′ (restriction sites underlined). The amplified insert was digested with *Bam*HI and *Eco*RI and cloned into the expression vector, pET28b (Novagen), to yield a construct encoding proEP-B2 with both N- and C-terminal His_6 tags. The resulting plasmid, pMTB1, was verified by DNA sequencing and introduced into *E. coli* BL21(DE3) (Novagen) via transformation. A 5 ml inoculum was grown for 12–16 hr by shaking at 37ºC. One liter of Luria-Bertani medium containing 50 μg/ml kanamycin was inoculated with the 5 ml inoculum and was grown at 37ºC. At an OD_{600} of 0.6, expression of recombinant proEP-B2 was induced by addition of 0.25 mM isopropyl β-D-thiogalactoside (Sigma). The culture was incubated at 37ºC for an additional 20 hr.

Induced cells were harvested by centrifugation at 5,000 × g for 20 min in a J2-21M Beckman centrifuge. The cell pellet was resuspended in 40 ml disruption buffer (200 mM sodium phosphate [pH 7.0], 200 mM NaCl, 2.5 mM DTT, 1.5 mM benzamidine, 2.5 mM EDTA, 2 mg/l pepstatin, 2 mg/l leupeptin, 30% (v/v) glycerol) and lysed by sonication with a Branson Sonifier 450. Lysed cells were centrifuged at 45,000 × g for 60 min. The proEP-B2 inclusion bodies contained in the pellet were rinsed twice with water, and solubilized by addition of 7 M urea, 50 mM Tris-Cl, 2 mM β-mercaptoethanol (βMCE) (pH 8.0). The protein solution was further clarified by centrifugation at 45,000 × g for 60 min, and the supernatant was bound to 10 ml 1:1::Ni-NTA resin:ethanol slurry (Qiagen) for 2 hr at 4ºC. The resin was packed into a column and washed with 7 M Urea, 50 mM Tris-Cl, and 2 mM βMCE (pH 8.0) until no protein was detected in the wash by Bradford assay. The bound protein was then eluted with 7 M Urea, 50 mM Tris-Cl, 2 mM βMCE, 200 mM imidazole (pH 8.0). Eluted fractions containing the desired protein, as assessed by SDS-PAGE, were dialyzed against 100 sample volumes of refolding/storage buffer (100 mM Tris-Cl [pH 8.0], 5 mM EDTA, 15% (v/v) glycerol, 2 mM βMCE) at 4ºC for 3 hr, followed by a second dialysis against a fresh portion of refolding buffer overnight. Alternatively, elution fractions containing the desired protein were diluted into refolding buffer to a final concentration of 30 μg/ml, gently agitated overnight at 4ºC, and concentrated again. The final protein concentration was determined by Bradford assay. Proenzyme preparations were stored at 0ºC on ice or at −20ºC in freezer.

Substrates

The chromogenic reference substrate Z-Phe-Arg-pNA (Bachem, CA, catalog number L-1242) was dissolved in 5% (v/v) DMSO in H_2O and was stored at −20ºC. The 33-mer gluten peptide (LQLQPFPQPQLPY PQPQLPYPQPQLPYPQPQPF) [4] was synthesized by using Boc/

HBTU chemistry on solid phase as previously described [41], purified by reverse-phase HPLC, and stored at −20ºC following lyophilization. For proteolytic assays, the peptide was resuspended in H_2O prior to use.

The expression and purification of recombinant α2-gliadin (GenBank accession number: AJ133612) was performed as described [4]. Purified and lyophilized α2-gliadin was stored at −20ºC until being dissolved in 0.1 M acetic acid for use in digestion assays. Dissolved α2-gliadin was stored at 0ºC on ice. Myoglobin from equine skeletal muscle (catalog number M-0630) was purchased from Sigma. For further details, see the Supplemental Data.

Activation of ProEP-B2

To visualize proEP-B2 activation, proEP-B2 was diluted into sodium phosphate (pH 6.0) or sodium acetate (pH 4.5) at 1 mg/ml final concentration at 25ºC. After a variable duration, an equal volume of sample and Laemmli buffer/βMCE were mixed, boiled 5 min, and analyzed via SDS-PAGE.

When determining the concentration dependence of proEP-B2 activation, 0.5–8 μM proEP-B2 was preincubated in 200 μl 250 mM sodium citrate buffer (pH 3.0). Following preincubation at 25ºC for varying length of time, 800 μl substrate was added to each sample for a final concentration of 50 μM Z-Phe-Arg-pNA and 0.1–1.6 μM preincubated proEP-B2 in 50 mM sodium citrate buffer (pH 3.0). Reaction progress was followed by monitoring A_{410} with a UV/Vis spectrometer (410 nm, 4 nm slit width; model Lambda 35, Perkin-Elmer). The reaction rate was measured from the initial slope of the A_{410} vs time plots and converted to V_o in μM/min with ε_{410} = 8800 $M^{-1}cm^{-1}$ for pNA.

Preparation of a Purified, Inhibited Mature EP-B2 Stock for Structural Studies

EP-B2 was prepared from proEP-B2 by fully activating ~1.5 mg/ml proEP-B2 to its mature form and then inhibiting the mature enzyme with 10 M equivalents of the covalent cysteine protease inhibitor, leupeptin (Acetyl-Leu-Leu-Arg-al; Sigma). Inhibited EP-B2 was purified by anion exchange chromatography, buffer exchanged into 10 mM Tris (pH 8.0) buffer, concentrated by filter centrifugation, and stored on ice until used. For further details, see the Supplemental Data.

Crystallization and Structure Determination of Mature EP-B2 Bound to Leupeptin

Inhibited EP-B2 was crystallized by hanging-drop vapor diffusion with 9.2 mg/ml mature EP-B2 with a reservoir of 1.36 M Li_2SO_4 and 0.10 M HEPES (pH 7.0). Crystals used in data collection were cryoprotected by transfer to the reservoir solution supplemented with 10% (v/v) glycerol and flash frozen in liquid nitrogen.

Diffraction data for the EP-B2-leupeptin complex crystal were collected at the Advanced Light Source (Lawrence Berkeley National Laboratory, Berkeley, CA) on beamline 8.3.1, and the structure of the EP-B2-leupeptin complex was solved by homology modeling followed by molecular replacement. The coordinates for the structure have been deposited in the Protein Data Bank (PDB code: 2FO5). For further details on crystallization, data collection and processing, and structure solution and refinement, see the Supplemental Data.

Comparison of ProEP-B2 and EP-B2 Susceptibility to Pepsin and Trypsin

To compare the relative susceptibility of proEP-B2 and EP-B2 to pepsin, 0.5 mg/ml proEP-B2 or EP-B2 (both in the presence of 1 mM leupeptin, to prevent autoactivation of proEP-B2 at pH 3.0) was incubated with pepsin (0.5 mg/ml) at pH 3.0. The reaction was quenched at designated time points, and the digestion products were analyzed via SDS-PAGE. Trypsin (0.5 mg/ml) digestions were identical, except that they were performed at pH 6.0 and that leupeptin was not added since proEP-B2 cannot autoactivate at this pH.

pH Dependence of Proenzyme Activation and Mature Enzyme Activity

To measure the pH optimum for the combined process, proEP-B2 was added to Z-FR-pNA at variable pH (2.3–6.9), and the rate of reaction was measured as above. To measure the effect of pH on only proEP-B2 activation, proEP-B2 was preincubated at variable pH (2.3–6.9) for 30 min at 25ºC. Thereafter, each reaction mixture was brought to pH 6.0, Z-FR-pNA was added, and the rate of reaction was measured as above. To measure the effect of pH on the catalytic activity of mature EP-B2, proEP-B2 was preincubated at pH 4.5 for 60 min at 25ºC. The assay mixtures were then adjusted to pH 2.3–6.9, Z-FR-pNA was added, and the rate of reaction was measured as above. In all pH dependence experiments, the final concentrations of enzyme and substrate were 0.4 μM and 50 μM, respectively. For further details, see the Supplemental Data.

EP-B2 Catalyzed Proteolysis of the 33-mer Gluten Peptide

Synthetic 33-mer peptide and proEP-B2 were added at final concentrations of 20 μM and 2 μM, respectively, to 50 mM sodium citrate (pH 3.0). These assay conditions were chosen because they promote rapid activation of the proenzyme and allow for catalytic activity by the mature enzyme. Control reactions contained no enzyme but were otherwise identical. After 60 min, 100 μl of the reaction mixture was injected onto a reversed-phase HPLC C_{18} column and eluted with a water-acetonitrile gradient containing 0.1% (v/v) TFA. An additional portion of reaction was quenched by boiling for 5 min and analyzed by LC-MS/MS.

EP-B2 Catalyzed Proteolysis of Recombinant α2-Gliadin and Bovine Myoglobin

Recombinant α2-gliadin and proEP-B2 were added at final concentrations of 50 μM and 4 μM, respectively, to 50 mM sodium citrate (pH 3.0) or to 50 mM sodium acetate (pH 4.5). Control reactions contained no enzyme but were otherwise identical. After a variable time period (5, 15, 30, and 60 min), a portion of the reaction mixture was quenched by boiling and analyzed by LC-MS/MS or, alternatively, added to an equal volume of Laemmli buffer/βMCE, boiled, and analyzed by SDS-PAGE. Spectral MS^2 data were searched against the SwissProt database with the Mascot online tool (Matrix Science), and α2-gliadin was correctly identified as the best hit. Those peptides with ion scores >30 were used to construct a cleavage map, and the frequency of each amino acid at substrate positions P5–P5′ flanking each cleavage site was tabulated and tested for significance with a statistical z test. For further details, see the Supplemental Data. Myoglobin digestions and cleavage site identifications were carried out under identical conditions to the α2-gliadin digestions at pH 4.5.

Supplemental Data

Supplemental data include two tables and additional Experimental Procedures and can be found with this article online at http://www.chembiol.com/cgi/content/full/13/6/637/DC1/.

Acknowledgments

This research was supported by R01 DK063158 to C.K. M.T.B. is a recipient of a National Institutes of Health Cellular and Molecular Biology Training Grant through Stanford University. We thank Dr. Tuan-Hua David Ho for providing the cDNA encoding *EPB2* and Dr. Lu Shan for performing the initial stages of subcloning *EPB2* into expression vectors. We also thank Andrew Guzzetta at the Stanford University Mass Spectrometry facility for his invaluable advice regarding sample preparation and data analysis. Dr. Axel T. Brunger is gratefully acknowledged for allowing use of his resources during crystal structure solution and refinement and for critical reading of the manuscript.

Received: November 7, 2005
Revised: April 4, 2006
Accepted: April 11, 2006
Published: June 23, 2006

References

1. Sollid, L.M. (2002). Coeliac disease: dissecting a complex inflammatory disorder. Nat. Rev. Immunol. *2*, 647–655.
2. Kagnoff, M.F. (2005). Overview and pathogenesis of celiac disease. Gastroenterology *128*, S10–S18.

3. Hausch, F., Shan, L., Santiago, N.A., Gray, G.M., and Khosla, C. (2002). Intestinal digestive resistance of immunodominant gliadin peptides. Am. J. Physiol. Gastrointest. Liver Physiol. *283*, G996–G1003.
4. Shan, L., Molberg, Ø., Parrot, I., Hausch, F., Filiz, F., Gray, G.M., Sollid, L.M., and Khosla, C. (2002). Structural basis for gluten intolerance in celiac sprue. Science *297*, 2275–2279.
5. Piper, J.L., Gray, G.M., and Khosla, C. (2004). Effect of prolyl endopeptidase on digestive-resistant gliadin peptides in vivo. J. Pharmacol. Exp. Ther. *311*, 213–219.
6. Marti, T., Molberg, Ø., Li, Q., Gray, G.M., Khosla, C., and Sollid, L.M. (2005). Prolyl endopeptidase-mediated destruction of T cell epitopes in whole gluten: chemical and immunological characterization. J. Pharmacol. Exp. Ther. *312*, 19–26.
7. Pyle, G.G., Paaso, B., Anderson, B.E., Marti, T., Li, Q., Siegel, M., Khosla, C., and Gray, G.M. (2005). Pre-treatment of food gluten with prolyl endopeptidase (PEP) avoids gluten-induced malabsorption in celiac sprue. Clin. Gastroenterol. Hepatol. *3*, 687–694.
8. Gass, J., Ehren, J., Strohmeier, G., Isaacs, I., and Khosla, C. (2005). Fermentation, purification, formulation, and pharmacological evaluation of a prolyl endopeptidase from *Myxococcus xanthus*: implications for celiac sprue therapy. Biotechnol. Bioeng. *92*, 674–684.
9. Fulop, V., Szeltner, Z., and Polgar, L. (2000). Catalysis of serine oligopeptidases is controlled by a gating filter mechanism. EMBO Rep. *1*, 277–281.
10. Shan, L., Marti, T., Sollid, L.M., Gray, G.M., and Khosla, C. (2004). Comparative biochemical analysis of three bacterial prolyl endopeptidases: implications for coeliac sprue. Biochem. J. *383*, 311–318.
11. Jacobsen, J.V., and Varner, J.E. (1967). Gibberellic acid-induced synthesis of protease by isolated aleurone layers of barley. Plant Physiol. *42*, 1596–1600.
12. Koehler, S.M., and Ho, T.-H.D. (1990). Hormonal regulation, processing, and secretion of cysteine proteinases in barley aleurone layers. Plant Cell *2*, 769–783.
13. Mikkonen, A., Porali, I., Cercos, M., and Ho, T.-H.D. (1996). A major cysteine proteinase, EPB, in germinating barley seeds: structure of two intronless genes and regulation of expression. Plant Mol. Biol. *31*, 239–254.
14. Davy, A., Svendsen, I., Sorensen, S.O., Sorensen, M.B., Rouster, J., Meldal, M., Simpson, D.J., and Cameron-Mills, V. (1998). Substrate specificity of barley cysteine endoproteases EP-A and EP-B. Plant Physiol. *117*, 255–261.
15. Vernet, T., Tessier, D.C., Laliberte, F., Dignard, D., and Thomas, D.Y. (1989). The expression in *Escherichia coli* of a synthetic gene coding for the precursor of papain is prevented by its own putative signal sequence. Gene *77*, 229–236.
16. Velasco, G., Ferrando, A.A., Puente, X.S., Sanchez, S.M., and Lopez-Otin, C. (1994). Human cathepsin O. Molecular cloning from a breast carcinoma, production of the active enzyme in *Escherichia coli*, and expression analysis in human tissues. J. Biol. Chem. *269*, 27136–27142.
17. Santamaría, I., Velasco, G., Pendás, A.M., Fueyo, A., and López-Otín, C. (1998). Cathepsin Z, a novel human cysteine proteinase with a short propeptide domain and a unique chromosomal location. J. Biol. Chem. *273*, 16816–16823.
18. Santamaría, I., Velasco, G., Pendás, A.M., Paz, A., and López-Otín, C. (1999). Molecular cloning and structural and functional characterization of human cathepsin F, a new cysteine proteinase of the papain family with a long propeptide domain. J. Biol. Chem. *274*, 13800–13809.
19. Serveau, C., Boulange, A., Lecaille, F., Gauthier, F., Authie, E., and Lalmanach, G. (2003). Procongopain from *Trypanosoma congolense* is processed at basic pH: an unusual feature among cathepsin L-like cysteine proteases. Biol. Chem. *384*, 921–927.
20. Brömme, D., Nallaseth, F.S., and Turk, B. (2004). Production and activation of recombinant papain-like cysteine proteases. Methods *32*, 199–206.
21. Than, M.E., Helm, M., Simpson, D.J., Lottspeich, F., Huber, R., and Gietl, C. (2004). The 2.0 Å crystal structure and substrate specificity of the KDEL-tailed cysteine endopeptidase functioning in programmed cell death of *Ricinus communis* endosperm. J. Mol. Biol. *336*, 1103–1116.
22. Stubbs, M.T., Laber, B., Bode, W., Huber, R., Jerala, R., Lenarcic, B., and Turk, V. (1990). The refined 2.4 angstroms X-ray crystal structure of recombinant human stefin B in complex with the cysteine proteinase papain: a novel type of proteinase inhibitor interaction. EMBO J. *9*, 1939–1947.
23. Choi, K.H., Laursen, R.A., and Allen, K.N. (1999). The 2.1 Å structure of a cysteine protease with proline specificity from ginger rhizome, *Zingiber officinale*. Biochemistry *38*, 11624–11633.
24. Baker, N.A., Sept, D., Joseph, S., Holst, M.J., and McCammon, J.A. (2001). Electrostatics of nanosystems: application to microtubules and the ribosome. Proc. Natl. Acad. Sci. USA *98*, 10037–10041.
25. DeLano, W.L. (2003). The PyMOL molecular graphics system (http://www.pymol.org/).
26. Turk, D., Guncar, G., Podobnik, M., and Turk, B. (1998). Revised definition of substrate binding sites of papain-like cysteine proteases. Biol. Chem. *379*, 137–147.
27. McGrath, M.E. (1999). The lysosomal cysteine endoproteases. Annu. Rev. Biophys. Biomol. Struct. *28*, 181–204.
28. Davy, A., Sorensen, M.B., Svendsen, I., Cameron-Mills, V., and Simpson, D.J. (2000). Prediction of protein cleavage sites by the barley cysteine endoproteases EP-A and EP-B based on the kinetics of synthetic peptide hydrolysis. Plant Physiol. *122*, 137–145.
29. Turk, D., Podobnik, T., Popovic, T., Katunuma, N., Bode, W., Huber, R., and Turk, V. (1995). Crystal structure of cathepsin B inhibited with CA030 at 2.0-Å resolution: a basis for the design of specific epoxysuccinyl inhibitors. Biochemistry *34*, 4791–4797.
30. Mach, L., Mort, J.S., and Glossl, J. (1994). Maturation of human procathepsin B. J. Biol. Chem. *269*, 13030–13035.
31. Vernet, T., Berti, P.J., de Montigny, C., Musil, R., Tessier, D.C., Menard, R., Magny, M.-C., Storer, A.C., and Thomas, D.Y. (1995). Processing of the papain precursor. J. Biol. Chem. *270*, 10838–10846.
32. Nykänen, M., Saarelainen, R., Raudaskoski, M., Nevalainen, K.M.H., and Mikkonen, A. (1997). Expression and secretion of barley cysteine endopeptidase B and cellobiohydrolase I in *Trichoderma reesei*. Appl. Environ. Microbiol. *63*, 4929–4937.
33. Saarelainen, R., Mäntylä, A., Nevalainen, H., and Suominen, P. (1997). Expression of barley endopeptidase B in *Trichoderma reesei*. Appl. Environ. Microbiol. *63*, 4938–4940.
34. Nykänen, M., Raudaskoski, M., Nevalainen, H., and Mikkonen, A. (2002). Maturation of barley cysteine endopeptidase expressed in *Trichoderma reesei* is distorted by incomplete processing. Can. J. Microbiol. *48*, 138–150.
35. Coulombe, R., Grochulski, P., Sivaraman, J., Menard, R., Mort, J.S., and Cygler, M. (1996). Structure of human procathepsin L reveals the molecular basis of inhibition by the prosegment. EMBO J. *15*, 5492–5503.
36. Fujishima, A., Imai, Y., Nomura, T., Fujisawa, Y., Yamamoto, Y., and Sugawara, T. (1997). The crystal structure of human cathepsin L complexed with E-64. FEBS Lett. *407*, 47–50.
37. Carmona, E., Dufour, E., Plouffe, C., Takebe, S., Mason, P., Mort, J.S., and Menard, R. (1996). Potency and selectivity of the cathepsin L propeptide as an inhibitor of cysteine proteases. Biochemistry *35*, 8149–8157.
38. Menard, R., Carmona, E., Takebe, S., Dufour, E., Plouffe, C., Mason, P., and Mort, J.S. (1998). Autocatalytic processing of recombinant human procathepsin L. J. Biol. Chem. *273*, 4478–4484.
39. Kalantzi, L., Goumas, K., Kalioras, V., Abrahamsson, B., Dressman, J.B., and Reppas, C. (2006). Characterization of the human upper gastrointestinal contents under conditions simulating bioavailability/bioequivalence studies. Pharm. Res. *23*, 165–176.
40. Arentz-Hansen, H., Korner, R., Molberg, Ø., Quarsten, H., Vader, W., Kooy, Y.M.C., Lundin, K.E.A., Koning, F., Roepstorff, P., Sollid, L.M., et al. (2000). The intestinal T cell response to α-gliadin in adult celiac disease is focused on a single deamidated glutamine targeted by tissue transglutaminase. J. Exp. Med. *191*, 603–612.

41. Xia, J., Sollid, L.M., and Khosla, C. (2005). Equilibrium and kinetic analysis of the unusual binding behavior of a highly immunogenic gluten peptide to HLA-DQ2. Biochemistry *44*, 4442–4449.
42. Sjöström, H., Lundin, K.E.A., Molberg, Ø., Korner, R., McAdam, S.N., Anthonsen, D., Quarsten, H., Noren, O., Roepstorff, P., Thorsby, E., et al. (1998). Identification of a gliadin T-cell epitope in coeliac disease: general importance of gliadin deamidation for intestinal T-cell recognition. Scand. J. Immunol. *48*, 111–115.
43. Molberg, Ø., McAdam, S.N., Körner, R., Quarsten, H., Kristiansen, C., Madsen, L., Fugger, L., Scott, H., Noren, O., Roepstorff, P., et al. (1998). Tissue transglutaminase selectively modifies gliadin peptides that are recognized by gut-derived T cells in celiac disease. Nat. Med. *4*, 713–717.
44. van de Wal, Y., Kooy, Y.M.C., van Veelen, P.A., Peña, S.A., Mearin, L.M., Papadopoulos, G., and Koning, F. (1998). Selective deamidation by tissue transglutaminase strongly enhances gliadin-specific T cell reactivity. J. Immunol. *161*, 1585–1588.
45. Molberg, Ø., McAdam, S.N., Lundin, K.E., Kristiansen, C., Arentz-Hansen, H., Kett, K., and Sollid, L.M. (2001). T cells from celiac disease lesions recognize gliadin epitopes deamidated in situ by endogenous tissue transglutaminase. Eur. J. Immunol. *31*, 1317–1323.
46. Arentz-Hansen, H., McAdam, S.N., Molberg, Ø., Kristiansen, C., and Sollid, L.M. (2000). Production of a panel of recombinant gliadins for the characterization of T cell reactivity in coeliac disease. Gut *46*, 46–51.
47. Vader, L.W., de Ru, A., van der Wal, Y., Kooy, Y.M.C., Benckhuijsen, W., Mearin, M.L., Drijfhout, J.W., van Veelen, P., and Koning, F. (2002). Specificity of tissue transglutaminase explains cereal toxicity in celiac disease. J. Exp. Med. *195*, 643–649.
48. Fleckenstein, B., Molberg, Ø., Qiao, S.W., Schmid, D.G., von der Mulbe, F., Elgstoen, K., Jung, G., and Sollid, L.M. (2002). Gliadin T cell epitope selection by tissue transglutaminase in celiac disease. Role of enzyme specificity and pH influence on the transamidation versus deamidation process. J. Biol. Chem. *277*, 34109–34116.
49. Siegel, M., Bethune, M.T., Gass, J., Ehren, J., Xia, J., Johannsen, A., Stuge, T., Gray, G.M., Lee, P.P., and Khosla, C. (2006). Rational design of combination enzyme therapy for celiac sprue. Chem. Biol. *13*, this issue, 649–658.

Accession Numbers

The coordinates for the structure of mature EP-B2 complexed with leupeptin have been entered into the Protein Data Bank under the accession number 2FO5.